



# Deep learning on field photography reveals the morphometric diversity of Colombian freshwater fish

Jose Luis Poveda-Cuellar<sup>1</sup> · David Morantes-Duarte<sup>2</sup> · Fabio Martínez-Carrillo<sup>2</sup> · Jorge Enrique García-Melo<sup>3</sup> · Sergio Marchant<sup>1</sup> · Björn Reu<sup>1</sup>

Received: 13 June 2025 / Revised: 10 September 2025 / Accepted: 26 September 2025  
© The Author(s) 2025

## Abstract

Neotropical freshwater fish are among the most morphologically diverse vertebrates; however, their study has long depended on preserved specimens, which limits our understanding of their natural body shapes due to preservation-induced distortions. Field photography provides a powerful, noninvasive alternative to capture the morphology of fish as it occurs in nature. However, automatically extracting accurate shape information from these images remains a major challenge, especially for highly diverse taxa. Here, we present an AI-based workflow that integrates Segment Anything and Grounding DINO to automate fish segmentation and shape extraction from field photographs. This approach enables a broad sampled analysis of the morphological diversity spectrum of Colombian freshwater fish. We applied this workflow to CavFish-Colombia, a curated dataset of 1749 images representing 78% of orders ( $n=11$ ), 82% of families ( $n=48$ ), 41% of genera ( $n=189$ ), and 25% of species/morphospecies ( $n=428$ ) of Colombian freshwater fish species, obtained using the PhotaFish standardized imaging system. Achieving more than 97% segmentation accuracy, our workflow enables precise and consistent extraction of natural fish body shapes. We provide the first structured morphospace of Colombian freshwater fish based on natural body shapes, quantified through descriptors such as area, perimeter, and invariant moments. This morphospace reveals distinct gradients in body size and outline related to locomotion and habitat use, spanning from large species with rounded shapes to small, elongate species. Most Colombian freshwater fishes share a predominant morphotype: small-bodied, laterally compressed. Deviations are order-specific, including Synbranchiformes that are elongate and slender; Characiformes, spanning deep-bodied and streamlined elongate types; and Siluriformes including small-bodied, streamlined, or dorsoventrally flattened armored shapes. Our results demonstrate that AI-driven field photograph analysis can allow for large-scale morphological studies, delivering accurate, rapid, and scalable data for biodiversity evaluations, functional trait analyses, and ecological research. This noninvasive morphological monitoring, directly from field images, opens new opportunities to assess fish morphology and analyze shape variation as it naturally occurs, capturing more accurate representations of living specimens.

**Keywords** Fish morphology · Foundation models · Field photography · Image-based morphometrics · PhotaFish system

## Introduction

Freshwater fish are one of the most diverse vertebrate groups globally (Tonella et al. 2023). Colombia hosts approximately 1711 species in several major hydrographic regions, including the Amazon, Orinoco, Caribbean, Magdalena-Cauca, and Pacific basins (DoNascimento et al. 2024). This notable biodiversity is crucial to maintaining the ecological integrity of freshwater ecosystems, serving as bioindicators of environmental health and contributing to essential processes such as nutrient cycling, habitat structure, and trophic interactions (Pelicice et al. 2023).

✉ Jose Luis Poveda-Cuellar  
josepovedaut@gmail.com

<sup>1</sup> Escuela de Biología, Universidad Industrial de Santander, Bucaramanga 680002, Colombia

<sup>2</sup> Escuela de Ingeniería de Sistemas e Informática, Universidad Industrial de Santander, Bucaramanga 680002, Colombia

<sup>3</sup> Facultad de Ciencias Naturales y Matemáticas, Programa de Biología Ambiental, Universidad de Ibagué, Ibagué 73001, Colombia

Moreover, this rich biodiversity is accompanied by high morphological diversity. Freshwater fish exhibit a wide range of shapes, sizes, and functional traits linked to various strategies for locomotion, feeding, reproduction, and habitat use (Gatz 1979; Winemiller 1991). Understanding this morphological diversity is crucial for assessing functional adaptations, species interactions, and the evolutionary processes that shape freshwater fish communities (Su et al. 2019). However, accurately capturing the morphological diversity of freshwater fish requires innovative measurement techniques that overcome the limitations of traditional morphometry (Saleh et al. 2023). Traditional methods, relying on manual measurements or landmark-based geometric morphometrics (Claude 2008), are time-consuming, prone to measurement errors, and require the physical handling of specimens (Saleh et al. 2023). Furthermore, the use of preserved specimens introduces biases due to morphological distortions caused by fixation and the preservation processes (Barragán et al. 2024), as such alterations complicate species comparisons and ecological interpretations (Martinez et al. 2013). Consequently, studies increasingly favour photographing live specimens in the field (Sotola et al. 2019; Barragán et al. 2024) or collecting high-quality images immediately after capture (García-Melo et al. 2019; Petrellis 2021). These approaches preserve each fish's natural shape in life, providing more reliable input for morphometric analyses.

Field photography has become a crucial tool in ichthyological research, offering a noninvasive and standardized approach to capturing taxonomically informative images of live fish (García-Melo et al. 2019). That is, advances in field photography systems (Sabaj Pérez 2009; García-Melo et al. 2019) now enable researchers to obtain high-resolution images with minimal handling, significantly reducing stress and mortality while preserving the natural colors, meristic traits, and morphometric characteristics of the specimens. However, unlike other vertebrates, fish remain among the least photographed organisms in the wild, largely due to the challenges of observing them in their natural habitats (García-Melo et al. 2019).

The integration of artificial intelligence (AI) tools, particularly computer vision and machine learning, offers a promising solution. AI-powered methods automate the measurement of morphometric traits, increasing the scalability and efficiency of data collection while reducing the need for manual processing (Ou et al. 2023; Bakış et al. 2023). These methods focus on two main tasks: detecting key anatomical landmarks and segmenting the fish body from an image. Landmark detection uses AI models to identify specific reference points, such as the snout, eye, and dorsal fin base, allowing for measurement of traits such as body length, height, and head size (Bakış et al. 2023; Saleh et al. 2023).

This process relies on deep learning techniques, including artificial neural networks (Bakış et al. 2023), convolutional neural networks (Tseng et al. 2020) such as the Mobile Fish Landmark Detection Network (Saleh et al. 2023), which incorporates elements of transformer-based architectures for improved efficiency. The second key task, body segmentation, allows AI to automatically outline the shape of the fish, facilitating the extraction of measurements such as total length, body width, and features of the tail and eyes (Fernandes et al. 2020; Ariede et al. 2023). Deep learning models like Mask R-CNN, SegNet, and U-Net (Fernandes et al. 2020; Yu et al. 2020) have been widely used for this purpose, providing high precision while reducing errors from manual tracing.

Despite recent advances, the widespread implementation of AI-based morphometrics in species-rich tropical ichthyofaunas remains constrained by five insufficiently developed areas of research and practice. First, there is taxonomic and geographic bias in the training data. The main public datasets, such as annotated image sets like DeepFish (Garcia-d'Urso et al. 2022) and FishAir (Bakış et al. 2023), are valuable starting points, but cover only a small fraction of the taxonomic and morphological diversity observed in Colombian freshwater fishes. Because they do not encompass the entire phenotypic spectrum, models trained exclusively on these datasets have difficulty generalizing Colombia's highly heterogeneous ichthyofauna (Ariede et al. 2023). Second, the absence of an open-access unified image repository for Neotropical fish. Scattered photographs lack standardized metadata, hindering the development of representative benchmarks for model training and evaluation across habitats ranging from Andean headwaters to Amazonian floodplains. Third, there is limited model generalization. Landmark-detection and segmentation networks such as Mask R-CNN and U-Net are typically tuned to single-species or laboratory image sets, raising questions about their accuracy on heterogeneous field photographs of non-model taxa (Fernandes et al. 2020; Tseng et al. 2020; Saleh et al. 2023). Fourth, limited representativeness of body shapes remains a constraint. Current AI-morphometric efforts have primarily targeted laterally compressed species with the typical complement of paired and unpaired fins (anal, caudal, dorsal, pectoral, pelvic), most notably characiforms. In contrast, the full spectrum of body plans, traits that are rarer, taxonomically variable, and of particular interest to biologists, such as the occurrence of multiple dorsal fins, the adipose fin, or barbels in freshwater fishes, remains largely unexplored, especially in Colombian ichthyofauna. Dorsoventrally flattened taxa such as Loricariidae, fusiform shapes (*Symbranchus marmoratus*), discoid rays (*Potamotrygon* spp.), and lineages lacking some paired and/or medial fins (*Eigenmannia* spp.) remain virtually

absent from training sets and benchmark studies. Consequently, current models cannot recognize or quantify the distinctive outlines that define these morphotypes, often focusing on commercially important marine fish (Yu et al. 2020; Han et al. 2022). Fifth, a lack of ecological validation, as no study has yet tested whether AI derived masks measured on live specimens, capture functionally important shape variation or explain patterns of morphospace occupancy. Collectively, these gaps limit the transferability and ecological relevance of AI-driven morphometric pipelines in the data-poor yet biodiversity-rich freshwater systems of the Neotropics.

To address these limitations, the Segment Anything Model (SAM) (Kirillov et al. 2023) presents a promising alternative for automated segmentation. Foundational models have gained significant attention in AI research as large-scale self-supervised learning frameworks capable of extracting generalizable representations without the need for extensive labelled datasets (Schneider et al. 2024). These models operate under unsupervised and weakly supervised training frameworks, allowing them to adapt to diverse contexts with high variability. SAM, trained on a vast data set containing more than 1 billion object masks derived from 11 million high-quality images (Kirillov et al. 2023), has demonstrated remarkable generalization capabilities across a wide range of biological taxa, effectively delineating anatomical structures such as fins, heads, and body outlines (Bakış et al. 2023). However, its application to Neotropical freshwater fish remains largely unexplored, and the accuracy and ecological relevance of SAM-generated segmentations for morphometric analyses require rigorous validation.

This study presents a novel framework for the automated characterization of Colombian freshwater fish, leveraging ensemble foundational models to improve generalization and ensure robust performance in diverse, uncontrolled environments. By photographing live fish directly in the field, this study captures undistorted, natural body shapes, providing a more accurate representation of morphological diversity. Additionally, by harnessing the power of ensemble foundational models, this study aims to achieve the automated quantification of morphometric traits in highly diverse freshwater fish assemblages, providing an ecologically relevant basis for ichthyological research. Furthermore, this study offers the first broadly sampled analysis of the spectrum of morphological diversity in Colombian freshwater fish, which contributes a valuable foundation for ecological and ichthyological research. The use of computed geometric moments supports quantitative morphometric assessment and facilitates interpretable, explainable analyses within the studied cohort.

## Materials and methods

### Study area

This study focuses on the freshwater fish assemblages of the cis and trans-Andean regions of Colombia. These regions encompass a high diversity of hydrographic basins, including the Magdalena, Cauca, Atrato, Sinú, Amazon, and Orinoco basins. These basins were selected due to their high species richness and the availability of georeferenced photographic records within the CavFish database (<https://cavfi.sh.unibague.edu.co>).

### CavFish-Colombia dataset

The Visual Catalog of Freshwater Fish in Colombia (CavFish-Colombia; <https://cavfish.unibague.edu.co>) is a curated repository of 1749 field photographs that collectively cover 78% of orders ( $n=11$ ), 82% of families ( $n=48$ ), 41% of genera ( $n=189$ ), and 25% of species/morphospecies ( $n=428$ ) recognized in national checklists (Table S2). Taxonomic representation is dominated by Characiformes, Siluriformes (e.g., Loricariidae), and Blenniiformes (e.g., Cichlidae), with smaller contributions from Synbranchiformes, Myliobatiformes, and Osteoglossiformes, a pattern characteristic of Amazonian ichthyofaunas in which Characiformes and Siluriformes are the most species-rich orders. This catalogue uniquely captures fish in their natural environments and, with photographic records from 2016 to 2023 includes specimens from the Magdalena-Cauca, Chocó Biogeográfico, Orinoco, and Amazon basins, highlighting Colombia's aquatic biodiversity. All images were obtained according to Colombian regulations and permits for biological collections.

### Image acquisition and standardization

CavFish photographs were obtained using the Photafish system (García-Melo et al. 2019), a standardized field photography set-up designed for ecological studies. All photographs were taken of live fish inside a portable aquarium, using either a white or black background, with or without a scale rule, under consistent lighting conditions. The CavFish/Photafish pipeline employs a modular imaging setup with aquaria of multiple sizes. For long, large, or deep-bodied species (e.g., *Pseudoplatystoma metaense*, *Pseudoprimelodus* sp.), we used a custom large tank built to preserve the same optical geometry (lighting, background, camera subject distance) and pose standardization as in the smaller tanks. This ensured that lateral views remained comparable across size classes and minimized distortions that could otherwise affect area and perimeter estimates. The cameras

(Canon EOS 70D, ILCE-7M3, ILCE-7RM4A, ILCE-6000) provided high-resolution images. Each image was accompanied by detailed camera metadata, including parameters such as approximate focus distance, image size, megapixels, field of view (FOV), focal length, sensor dimensions, and crop factor. In addition, species were identified by expert ichthyologists, and species names were standardized and classified according to their respective families, following Colombia Checklist V.2.17 (DoNascimento et al. 2024).

The fish were photographed in a left-lateral view with a straight body axis, and all external structures (fins, eye, barbels) were clearly visible, avoiding any occlusion. We then manually screened CaVFish images and excluded those that could bias area or perimeter, such as incomplete bodies, torn or missing fins, strong body curvature or deviations from a true lateral view. Similarly, we prioritized adult individuals to minimize morphometric variation associated with ontogenetic development, excluding juvenile specimens whenever possible. The size of the fish was estimated in millimeters by converting the measurements of the pixels using a scale rule (10 mm) present in the images, determining the number of pixels corresponding to 10 mm. This ratio enabled for accurate pixel-to-millimeter conversion. Then, the size of the fish was estimated by multiplying the number of pixels occupied by the fish by the corresponding conversion factor.

## Data processing pipeline

We adapted state-of-the-art computer-vision methods, originally developed for generic or natural object segmentation, to process field photographs of live fish and translate them into ecologically meaningful measures of shape variation.

The workflow proceeds through four logically ordered stages (Fig. 1). (1) Segmentation: deep-learning models first detect each specimen and generate a high-resolution mask that cleanly separates fish from the background. (2) Morphometric validation: overlap and shape-agreement metrics benchmark those masks against expert annotations, ensuring that only high-fidelity segmentations advance. (3) Descriptor extraction: from every validated mask, we calculate size and shape sensitive metrics (area, perimeter, Hu and Zernike moments, etc.) that capture the biologically relevant dimensions of fish morphology. (4) Morphometric-diversity analysis: multivariate ordination and kernel-density mapping project these descriptors into a reduced trait space, revealing the structure of interspecific morphological variation and delineating the empirical morphospace. Together, these stages convert raw imagery into rigorously validated quantitative data suitable for ecological inference.

### 1. Segmentation of fish

The segmentation of fish images is achieved using a two-step pipeline incorporating two deep learning models, Grounding DINO (Liu et al. 2024) and the SAM (Kirillov et al. 2023). These models allow for automatic fish detection and precise shape localization in images, a crucial step for morphometric analyses. Automatic detection with Grounding DINO, an object detection model that identifies and coarsely bounds the fish shape into a rectangle within an image by combining two sources of information: text-based descriptions (e.g., the word “fish”) and visual features extracted from the image. It should be noted that, in this study, the fish detection is mainly related to visual features, following

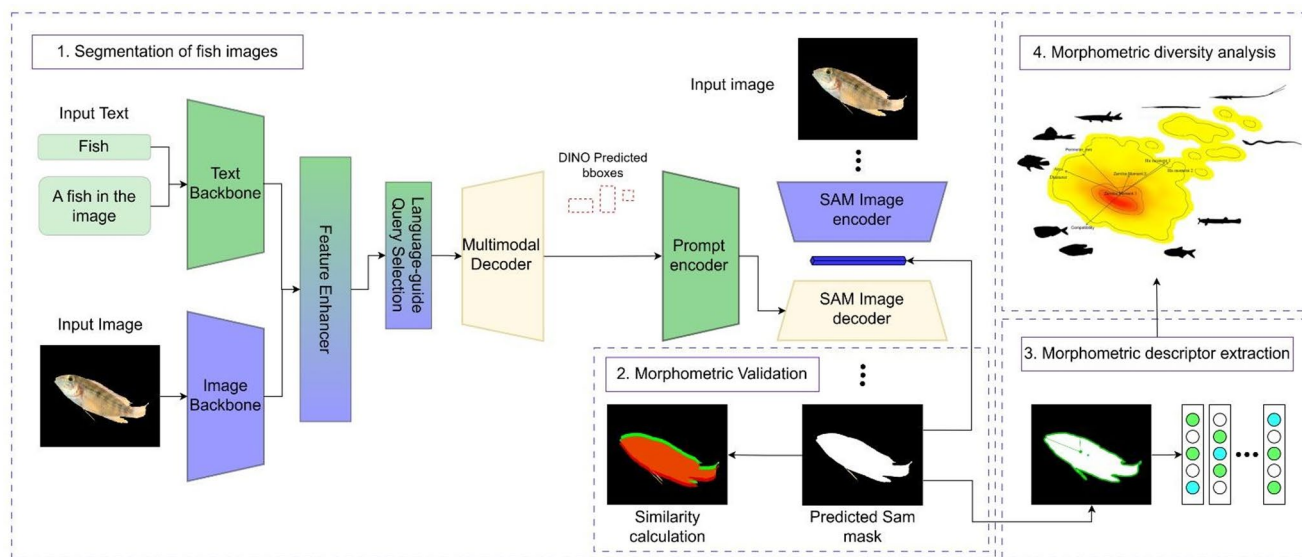


**Fig. 1** Methodological workflow: (1) Segmentation of fish images using DINO and SAM, (2) Morphometric Validation, (3) Morphometric descriptor extraction, and (4) Morphological diversity analysis

unique and general prompts that avoid any interference in the final results. The Grounding DINO employs an ensemble of vision-transformer blocks to analyze visual features. Each transformer splits the image into a set of subregions that preserve spatial information with positional embeddings analyzed through an attention mechanism. In AI, such attention mechanisms have demonstrated strong capabilities to recover complex and nonlocal patterns, allowing for more efficiency in training tasks, such as the detection of objects. Each transformer module is then coupled in series, extracting from coarse to fine image features such as shapes, texture, and color patterns. Consequently, Grounding DINO can perform precise localization of each fish in an image with exceptional accuracy.

To improve the detection ability, Grounding-DINO was fine-tuned using the FishNet dataset (Khan et al. 2023), which includes 94,532 images from 463 fish families captured in various orientations, habitats, and environmental conditions. Optimization used predefined parameters, including image scaling (400–600 px) to preserve detail while minimizing distortion. Feature extraction used a Swin-T-based encoder with spatial corrections, plus a 6-layer transformer network to focus on key regions. Training lasted 30 epochs with AdamW, adjusting learning rates for stability and to prevent overfitting. Once detected, Grounding-DINO outputs a bounding box defining the segmentation region. In our methodology, we only perform pre-training of Grounding-DINO on the FishNet dataset, which was partitioned 70% for training, 10% for validation, and 20% for testing. Subsequently, we validated the full pipeline at inference time using a second, in-house dataset with expert manual annotations.

For morphometric analysis, the SAM isolates the fish from the background to achieve a precise segmentation of the fish body. A key advantage of SAM is its prompt-based adaptability, allowing it to segment objects in new image types without requiring additional training, an aspect we leverage directly without further fine-tuning. For this, SAM operates through three main components: the prompt encoder, the image encoder, and the image decoder. Because we gave every image exactly the same prompt, the prompt encoder did not influence the final masks. Segmentation therefore depended only on the image encoder and mask decoder, and our evaluation focuses on how well these two modules segment each fish. The bounding boxes produced by Grounding DINO are first processed by the Prompt Encoder, which interprets them as instructions for segmentation. The image encoder then extracts relevant features from the entire image, capturing information about texture,

shape, and contrast. Similarly to the basic DINO, the SAM model incorporates an encoder with multiple transformer modules. From the set of ensemble encoder transformers, there are output embedding vectors that are complex descriptors with the most salient image features. These vectors are mapped to a decoder, also formed by ensembles of transformers, but dedicated to retrieving segmentation. The image decoder generates a precise segmentation mask, effectively isolating the fish from other objects in the image. Additionally, to improve segmentation quality and ensure seamless, well-defined boundaries, morphological transformations such as opening and closing are applied. These operations effectively eliminate gaps and discontinuities within the masks, smooth the segmented regions, and remove small artefacts, resulting in a more precise and continuous representation of the fish body.

## 2. Morphometric validation

### 2.1. Manual annotations for segmentation validation

To ensure the precision of the segmentation results, 1,749 fish images were manually annotated using the Computer Vision Annotation Tool (CVAT). These annotations precisely delineated the fish boundaries, providing a high-fidelity representation of the shape of the fish and serving as a benchmark for comparison with SAM-generated segmentations.

### 2.2. Segmentation performance and statistical error assessment

To quantify the accuracy of segmentations generated by the SAM, the following metrics were employed: Intersection of Union (IoU) and the Dice coefficient. The IoU measures the overlap between the predicted segmentation mask and the manually annotated ground-truth mask, normalized by their union. It is calculated as

$$\text{IoU} = \frac{\text{Area of Intersection}}{\text{Area of Union}}$$

where IoU quantifies the proportion of spatial overlap between the two masks and ranges from 0 (no overlap) to 1 (perfect overlap). A value of 1 indicates that the model reproduced the ground-truth segmentation exactly.

The Dice coefficient, also known as the F1 score, assesses the similarity between the predicted masks and the ground truth masks. It is calculated as

$$\text{Dice} = 2 * \frac{\text{Area of Intersection}}{\text{Area of Predicted} + \text{Area of Ground Truth}}$$

where a Dice coefficient of 1.0 indicates perfect agreement and 0.0 indicates no agreement.

To characterize the distribution of segmentation errors, we modelled the IoU and Dice coefficient values using a Beta distribution. The Beta distribution is appropriate for modelling bounded data, such as the IoU and Dice coefficients, which range from 0 to 1. The mean and standard deviation of the Beta distribution were estimated for both metrics. To define an error range, the thresholds of three standard deviations from the mean were calculated. Segments with IoU or Dice values falling outside this range were flagged as potential errors, indicating significant deviations from the expected segmentation accuracy. This approach allowed for the identification of outliers and ensured that the segmentation results met predefined accuracy criteria.

### 2.3. Validation of segmentation accuracy using morphometric metrics

We assessed segmentation fidelity by comparing the area (number of pixels classified as fish) and the perimeter (length of the predicted outline) against their manual counterparts. These two first-order measurements are the building blocks of every shape descriptor used later in the study. Derived variables, such as equivalent diameter, compactness, and the families of Hu and Zernike moments, are mathematically expressed as functions of area and perimeter alone (Hu 1962; Gonzalez and Woods 2018). Consequently, if the model reproduces the area and perimeter with high precision, the accuracy of all metrics that depend on them follows directly. Validating these foundational quantities therefore provides a concise, yet rigorous, quality check, sparing the need to repeat the exercise for each individual higher-order descriptor while still ensuring the integrity of downstream morphometric analyses. The agreement between predicted and observed morphometric values was assessed using the following metrics: Root Mean Square Error (RMSE), Coefficient of Determination ( $R^2$ ), and Residual Prediction Deviation (RPD). The RMSE quantifies the average magnitude of the errors between the predicted and observed values, providing an absolute measure of prediction accuracy. It is calculated as  $RMSE = \sqrt{\text{mean}((\text{predicted} - \text{observed})^2)}$ . The  $R^2$  measures the proportion of variance in the observed values that is predictable from the predicted values, indicating the goodness of fit of the model. The RPD contextualizes the RMSE by comparing it to the standard deviation of the observed values, providing a measure of predictive performance relative

to the variability of the data. It is calculated as  $RPD = \text{standard deviation (observed)} / \text{RMSE}$ . RPD values greater than 2 indicate acceptable predictive performance, while values greater than 3 suggest excellent performance (Helser et al. 2019).

### 3. Morphometric descriptor extraction

After rescaling each 2-D image so that pixel equals millimeter, we extracted a broad set of morphometric descriptors from the segmentation masks to quantify fish body shape. The descriptors included area, perimeter, diameter, compactness, and Hu and Zernike moments (Hernández-Serna and Jiménez-Segura 2014). Normalization ensures that measurements are consistent and comparable across images, regardless of variations in the original image size or resolution. Evaluation of the results obtained from AI-based segmentation against established morphometric descriptors aimed to validate the accuracy and reliability of automated approaches to capture meaningful shape variations between diverse species of fish. Each descriptor captures specific aspects of fish morphology, providing a robust quantitative framework for comparing species with different body shapes and structural features. Detailed information on each descriptor is provided in Table 1, and visual representations are shown in Figure S1 in Supporting Information.

### 4. Morphometric diversity analysis

To analyze the morphometric variation between fish species in the dataset, Principal Component Analysis (PCA) was applied to the extracted descriptors. PCA reduces the dimensionality of the feature space, identifying the principal axes of variation, and enabling visualization of species clustering based on their morphometric characteristics. The analysis was performed on the correlation matrix. All analyses focused on the first four principal components, and were evaluated for every 2-D pairing among them: PC1-PC2, PC1-PC3, PC1-PC4, PC2-PC3, PC2-PC4, and PC3-PC4. Before analysis, the distribution of each variable was examined and logarithmic  $x+1$  transformations were applied to approximate normality. After transformation, the variables were standardized using z-transformation to ensure equal contribution to PCA. Furthermore, Pearson's correlation coefficient was calculated to assess the strength of the relationships between variables, helping to identify potential multicollinearity.

To characterize species distributions in the morphospace beyond the variance explained, we assigned each species to one of four sign-defined quadrants for every pairwise combination of the first four PCs (PC1-PC4): ++, +-, -+, and --. For each PC pair, we estimated the

**Table 1** Morphometric descriptors for shape analysis in fish

Descriptor	Meaning	Higher value	Lower value
Area	Total region occupied by the fish in the image, approximating body size.	Larger-bodied species with broad shapes and well-developed fins (e.g., <i>Aequidens</i> sp. Eigenmann and Bray 1894).	Smaller-bodied, streamlined species (e.g., <i>Belonion dibranchodon</i> Collette 1966).
Perimeter	Length of the fish's contour, reflects the complexity of the boundary.	Irregular outlines with extended fins, barbels, or odontodes (e.g., <i>Ctenolucius hujeta</i> (Cuvier and Valenciennes 1850)).	Compact bodies with smooth outlines (e.g., <i>Synbranchus marmoratus</i> Bloch 1795).
Diameter	Estimated width, assuming a circular equivalent shape based on area.	Broad, deep-bodied species (e.g., <i>Serrasalmus hollandi</i> Eigenmann 1915).	Narrow, elongated species (e.g., <i>Belonion dibranchodon</i> Collette 1966).
Compactness	The relationship between area and perimeter indicates shape roundness.	More circular, symmetrical bodies (e.g., <i>Heros severus</i> Heckel 1840).	Elongated or irregularly shaped species (e.g., <i>Farlowella mariae</i> Martín Salazar 1964).
Hu moments	Shape descriptors invariant to translation, rotation, and scaling.	Asymmetrical or highly elongated species (e.g., <i>Synbranchus marmoratus</i> Bloch 1795).	Symmetrical species (e.g., <i>Poptella compressa</i> (Günther 1864)).
Zernike moments	Orthogonal shape descriptors capturing morphological complexity.	Finer structural details, such as barbels, odontodes, or fin extensions (e.g., <i>Poptella compressa</i> (Günther 1864)).	Streamlined, elongated bodies with fewer localized features (e.g., <i>Triplotheus</i> sp.).

proportion of species in each quadrant, and quantified uncertainty with a nonparametric bootstrap ( $B=1,000$ ) to derive the percentile 95% confidence intervals. We then repeated these counts within each taxonomic Order to obtain within-Order quadrant proportions for every PC pair, enabling comparison of dominant morphotypes among clades. Finally, to link occupancy to underlying morphology, we computed the mean standardized (z-score) of each morphometric variable within every quadrant and PC pair and summarized these signatures as heatmaps to identify trait shifts across regions of the morphospace.

To further explore the distribution of fish species within the morphospace, we applied Kernel Density Estimation

(KDE) to the PCA-transformed data. To estimate the probability of occurrence for morphometric descriptors within a two-dimensional space defined by the first two principal component (PC) axes, two-dimensional KDE (Carmona et al. 2024) was utilized. Given that kernel density estimates are sensitive to the choice of smoothing bandwidth, unconstrained bandwidth selectors (Duong 2007) were employed to optimize the analysis. In this approach, the bandwidths for individual groups (e.g., taxonomic orders) were constrained by the overall bandwidth of the data set to ensure that the density estimates for each group remained within the morphometric descriptor space defined by the entire dataset. To visualize the probability distribution of trait combinations across the PCA space, contour plots were generated based on the two-dimensional kernel density distributions. These plots employed a color gradient and contour lines to represent the 0.5, 0.95, and 0.99 quantiles of the probability distribution, thus highlighting areas with the highest and lowest probabilities of occurrence for specific morphometric descriptors.

All analyses were performed on high-performance workstations equipped with NVIDIA GPUs to accelerate deep learning model training and evaluation. The development and analysis were carried out using Jupyter Notebook in Google Colab, and deep learning frameworks such as TensorFlow and PyTorch (Paszke et al. 2019) were used to implement the models. The extraction of morphometric features was performed using custom image processing scripts, while KDE and PCA analyses were carried out using the funspace R package (Carmona et al. 2024).

## Results

### Segmentation process

The segmentation process demonstrated high accuracy, with a mean Dice coefficient of 0.98 and a mean IoU of 0.97. Both metrics exhibited narrow distributions around their respective means. The standard deviation (SD) thresholds of the Dice coefficient were  $\pm 1$  SD (0.91),  $\pm 2$  SD (0.95), and  $\pm 3$  SD (0.97). Similarly, the IoU thresholds were:  $\pm 1$  SD (0.89),  $\pm 2$  SD (0.93), and  $\pm 3$  SD (0.97) (Fig. 2). These results indicate consistent and highly accurate segmentation, achieving approximately 98% agreement with manual annotations.

A statistical threshold analysis using a Beta distribution identified potential segmentation errors. Outliers, detected as values exceeding  $\pm 3$  SD from the mean, and Dice values

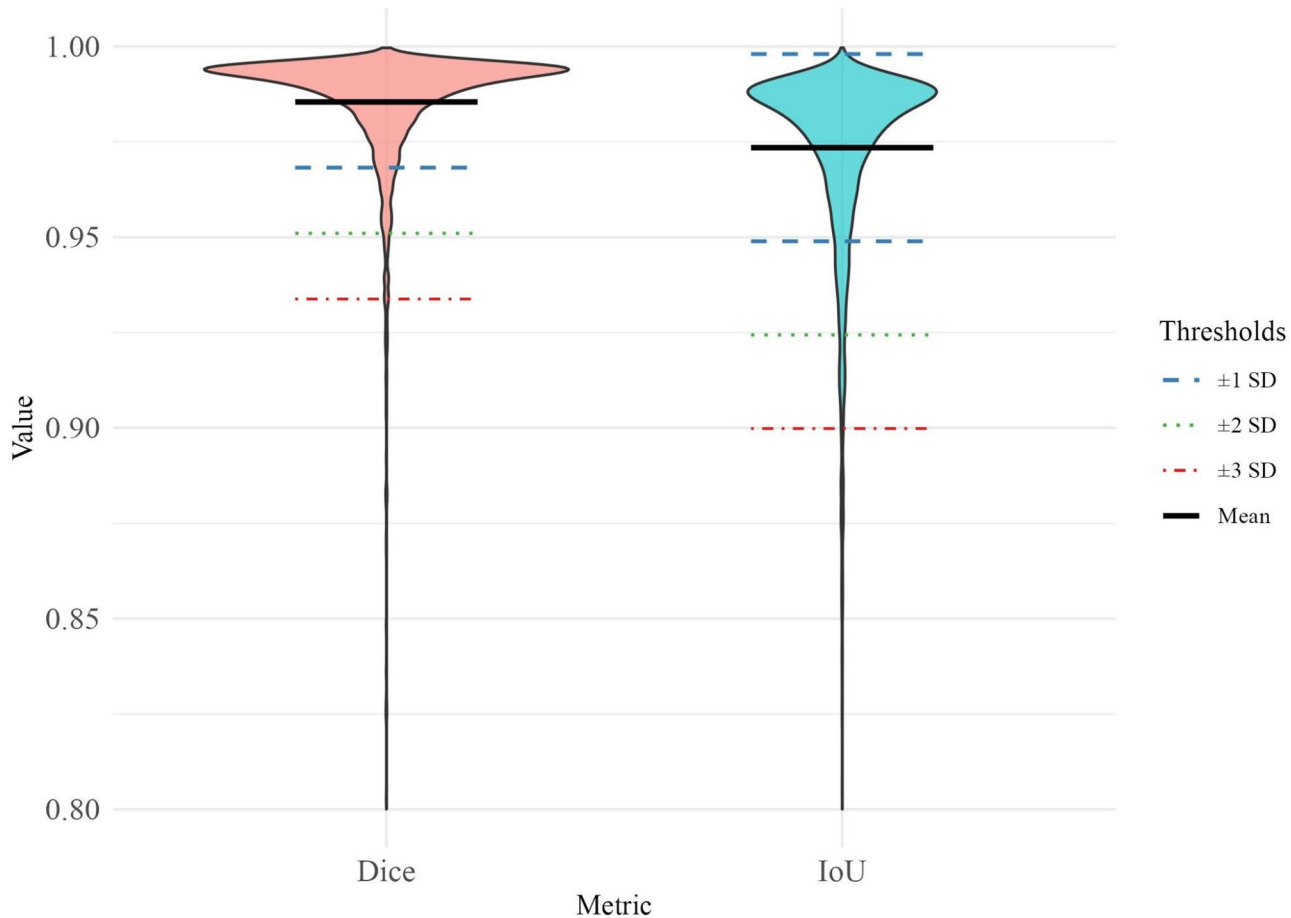


**Fig. 2** Distribution of dice and IoU metrics for fish segmentation performance

below 0.91 and IoU values below 0.89 (Fig. 2). These outliers represented only 29 images, or 1.6% of the total dataset (Fig. S2), suggesting a low error rate for the segmentation process.

### Morphometrics trait extraction accuracy

The accuracy of the extracted morphometric measurements was assessed by comparing the observed and predicted values for the area of the fish ( $\text{px}^2$ ) and the perimeter (px). The prediction model exhibited strong predictive performance, with an  $R^2$  of 0.995 for the area and 0.945 for the perimeter (Fig. 3), indicating excellent agreement between the predicted and observed values (see details in the supporting information, Fig. S3).

The RMSE was calculated to quantify the accuracy of the prediction. The mean observed area was 2,922,600.91  $\text{px}^2$ , with an RMSE of 162,464.64  $\text{px}^2$ , representing 5.56% of the observed mean. The mean observed perimeter was 11,352.11 px, with an RMSE of 1,436.89 px, representing 12.66% of the observed mean. The higher relative RMSE for the perimeter may be attributed to increased sensitivity

to boundary delineation or data variability. Given that area is a squared measure, small inaccuracies in boundary delineation result in larger cumulative errors compared to perimeter, which is a linear measure.

The RPD was calculated to contextualize RMSE relative to the variability of the observed values. The RPD for the area was 14.695, and for the perimeter was 3.721. These values indicate a high predictive capacity for both measurements, with greater precision in area estimation compared to the perimeter (Fig. 3).

### Morphometric diversity analysis

The PCA revealed that 93% of the morphometric variation between the Colombian freshwater fish species is captured within the first four principal components (PCs) (Fig. 4, details in supporting information, Fig. S4, Table S1), indicating that these axes capture the dominant aspects of body shape. PC1 (41.7%) represents a gradient of species with large body areas and rounded outlines, such as *Serrasalmus* sp. (Characiformes), to those with smaller body areas and elongated outlines, as exemplified by *Synbranchus*

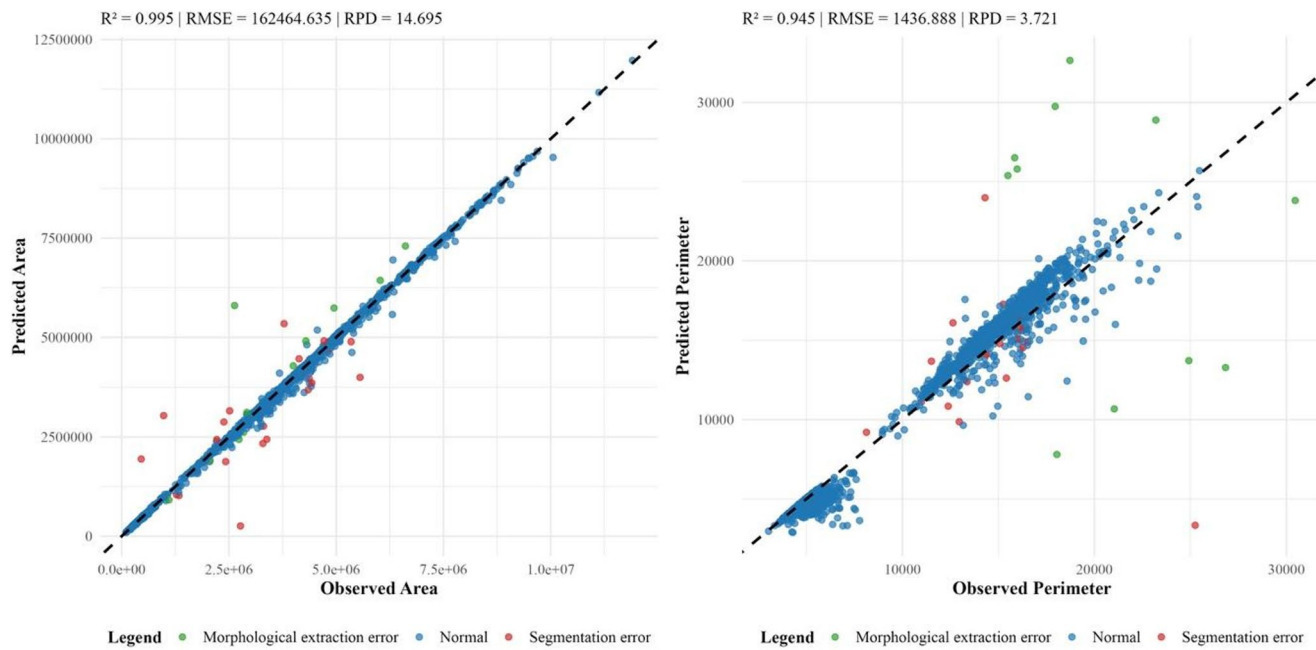


**Fig. 3** Observed versus predicted values for the 2D area and perimeter of the fish. The red points indicate outlier segmentations, and the green points indicate outlier perimeter values. The  $R^2$  and RMSE values indicate the accuracy of the predictions

*marmoratus* (Synbranchiformes). This axis reflects fundamental differences in body shape and size.

The PC2 (27.4%), primarily associated with perimeter, distinguishes species with large, irregular outlines from those with smaller, symmetrical outlines. This axis highlights the significance of proportionality and outline irregularity (see supporting information, Table S1). Species with higher perimeter values exhibit extensive fin structures, such as the well-developed dorsal fins in *Aequidens* and *Geophagus*, or elongated caudal fin rays seen in certain Siluriformes, particularly Loricariidae (e.g., *Hypostomus*). On the contrary, species with lower perimeter values typically display reduced fin structures, with some fins absent, short, or highly reduced, as observed in certain Trichomycteridae, where barbels and other appendages are minimal or absent.

The PC3 (12.5% of variance), which is most strongly associated with Zernike moment 1, contrasts deeper, rounder bodies, often with body structure such as dorsal-fin filaments (e.g., *Gasteropelecus* spp., *Myloplus* spp.), with more streamlined shapes (e.g., *Triplophysa* spp., *Acestrorhynchus* spp.). In turn, PC4 (11.5%), which is primarily associated with Zernike moment 3, separates streamlined taxa bearing fin extensions, including caudal-fin filaments (e.g., *Sturisomatichthys leightoni*), from strongly elongate species (e.g., *Synbranchus marmoratus*).

Using a nonparametric bootstrap, we identified the most filled quadrants for each PC pair (quadrant order on the x-axis: --, -+, +-, ++). For PC1-PC2, the +- quadrant

contains the highest proportion of species (30.9%, 95% CI), followed by -- and +- (both ~25%), whereas ++ is least common (18.5%). For PC1-PC3 and PC1-PC4, proportions are nearly uniform across quadrants (24–26% each), indicating no dominant sign combination, this indicates a balanced representation of the major shape captured by these axes, with species distributed in similar proportions across quadrants. In contrast, for PC2-PC3 and PC2-PC4, the -- quadrant dominates (29–31%), and the least frequent quadrant is +- for PC2-PC4 or ++ for PC2-PC3 (~19–22%). These differences are supported by the 95% percentile confidence intervals.

The standardized mean heatmaps the PC1- PC2 plane summarize the typical morphological profile of each region of morphospace. The -- quadrant (PC1-, PC2-) groups species with higher compactness and lower Hu moments; that is, rounder, deeper, and more symmetrical outlines, such as *Heros severus* and *Roebooides* spp. The -+ quadrant (PC1-, PC2+) shows a higher average area, perimeter, and diameter, but a lower Hu moment 1, such as *Geophagus steindachneri* and *Hypostomus* spp. The +- quadrant (PC1+, PC2-), which has the highest proportion of species, exhibits a lower average area, perimeter, and diameter, including small-bodied taxa such as *Creagrutus* spp., *Astroblepus* spp., and *Hemibrycon* spp. Finally, the ++ quadrant (PC1+, PC2+) is characterized by higher Hu moments and lower compactness, elongated outlines with relatively small areas, such as *Ctenolucius hujeta* and *Synbranchus marmoratus*. Similar trait patterns were observed in other component planes (e.g.,

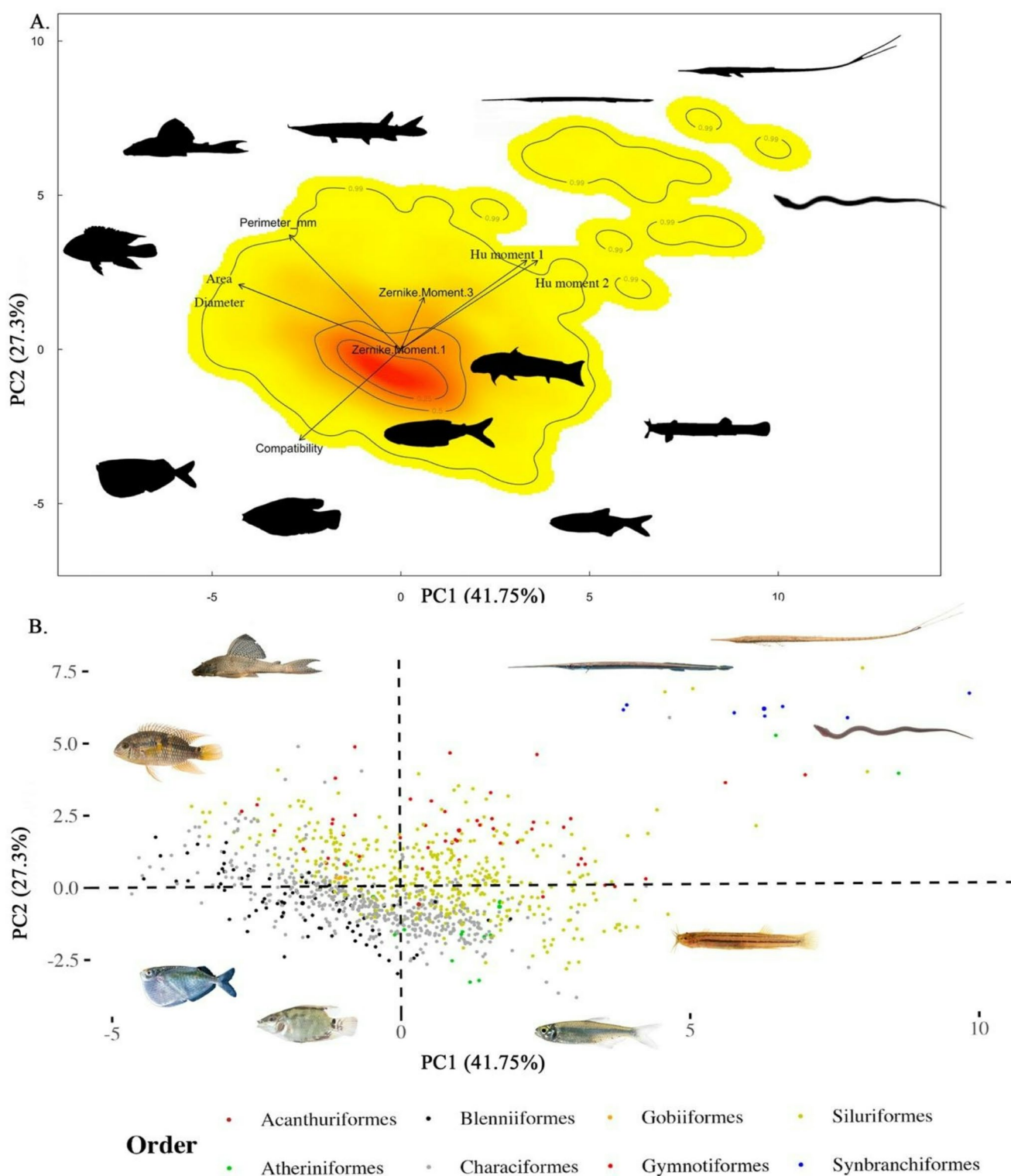


**Fig. 4** Morphometric diversity of Colombian freshwater fish. **A** Projection of Colombian freshwater fish (dots) onto the plane defined by the first two principal components (details in supporting information, Table S1). The color gradient represents the probability of species

occurrence, from highest (red) to lowest (white), with contour lines marking the 0.5, 0.95, and 0.99 quantiles (see Methods, KDE). Red regions within the 0.50 probability threshold indicate morphometric hotspots. **B** Distribution of taxonomic orders within the morphospace

PC1-PC3, PC2-PC3), although these axes show less separation among morphological profiles, suggesting that these morphological associations are consistent across multiple dimensions of morphospace.

Overall, the morphometric space of Colombian freshwater fish is dominated by a single high-density node, suggesting that most species share a common body shape (Fig. 2A). Located near the origin of the principal-component plot, this cluster contains intermediate-sized species with flattened, roughly elliptical bodies that are compressed either dorsoventrally or laterally. These species exhibit intermediate values for the Zernike moments and the Hu moments, reflecting relatively symmetric body shapes and moderate fin development. This group is predominantly composed of Characiformes, Siluriformes, Atheriniformes, and Blenniiformes, including species such as *Hemibrycon* spp., *Astroblepus* spp., *Andinoacara* spp., and *Chaetostoma* spp.

Morphospace occupancy shows orders with a single predominant morphotype and others spanning multiple body shapes (Supporting Information, Fig. S5). Synbranchiformes are concentrated in the ++ quadrant and exhibit elongate, slender bodies with relatively small areas and high Hu moment values (e.g., *Synbranchus marmoratus*). Acanthuriformes predominate in +-, consistent with small-bodied outlines. In contrast, species-rich Blenniiformes, Characiformes, and Siluriformes occupy multiple quadrants, indicating broad morphological diversity. Blenniiformes are mainly located in the - quadrant (rounder, deeper, and more symmetrical), marked by compact bodies and prominent fins (e.g., deep, laterally compressed profiles with elongated rays in the dorsal, caudal, and anal fins). Characiformes are largely distributed between the -- and +- quadrants (small-bodied shapes), with additional representation elsewhere. This variation spans from deep-bodied species with the full complement of paired and unpaired fins (e.g., *Serrasalmus hollandi*, *Heros severus*) to highly streamlined taxa such as *Ctenolucius hujeta*. Siluriformes display at least three prevalent shapes: ++ (elongate), +- (small-bodied), and -+ (streamlined with prominent fins), underscoring exceptional diversity. They represent the broadest morphometric concentration, encompassing both streamlined and dorsoventrally flattened shapes, such as *Lasiancistrus* spp. Likewise, Gymnotiformes occur across +-, -+, and ++, with long anal fins and slender, specialized morphotypes being especially common. In summary, the fauna shows a dominant body plan shared by many Colombian freshwater fishes, alongside distinct, order-specific and species-specific morphologies. These patterns highlight orders with unique body shapes (e.g., Synbranchiformes) and orders spanning several morphotypes (e.g., Characiformes, Siluriformes), reinforcing the heterogeneity of Colombian freshwater fish morphology.

## Discussion

Morphometric diversity is fundamental to understanding evolutionary trajectories, ecological adaptations, and species conservation, as morphology directly influences locomotion, feeding strategies, and habitat use (Gatz 1979; Winemiller 1991). This study represents the first large-scale morphological characterization of Colombian freshwater fish, analyzing 25% ( $n=428$ ) of 1,711 species of Colombian freshwater fish distributed in Magdalena-Cauca, Chocó Biogeográfico, Orinoco, and Amazon basins using an automated deep learning approach.

The methodology used integrates a two-step deep learning pipeline, with the SAM playing a key role in segmenting fish from field images. The ability of SAM to generalize across a wide range of body shapes, sizes, and pigmentation patterns makes it particularly valuable for large-scale studies (Kirillov et al. 2023). This segmentation enables the precise extraction of morphometric traits, including area, perimeter, and invariant moments. SAM achieved more than 97% segmentation accuracy, demonstrating its potential to replace manual segmentation and streamline morphometric analyses.

Although deep learning applications in fish segmentation have predominantly focused on marine and commercially important species, freshwater taxa have been largely underrepresented. Models such as SegNet (Fernandes et al. 2020) and Mask R-CNN (Ariëde et al. 2023) have been used in fewer than 60 freshwater species (Yu et al. 2020; Garcia-d'Urso et al. 2022; Rocha et al. 2024), primarily due to the scarcity of annotated image datasets. Traditional models require extensive manual labelling of body regions and keypoints (Hasegawa and Nakano 2024), limiting their adaptability to species with diverse morphologies and complex pigmentation patterns (Ariëde et al. 2023). A major challenge in fish segmentation research is the difficulty of generalizing models to morphologically distinct species, particularly in complex environmental backgrounds (Zhuang et al. 2021). The SAM overcomes this limitation through its zero-shot segmentation capability, delineating fish morphology without requiring species-specific labelled data (Schneider et al. 2024). This capability has been validated across various biological groups, including marine organisms (Hong et al. 2024), nematodes (Sigurðardóttir et al. 2024), and fish (Hasegawa and Nakano 2024), confirming its utility. This is the first study to apply SAM to an image data set standardized and annotated by ichthyologists, demonstrating its suitability for freshwater fish morphological analyses.

Despite its high accuracy, SAM exhibited segmentation errors in three main scenarios: (1) misclassification of non-biological elements when fish were positioned near aquarium walls or the water surface (see details in Supporting

Information, Fig. S2 A–C), (2) occasional omission of fine morphological structures such as barbels and small fins (see details in Supporting Information, Fig. S2 E), and (3) focusing on a single individual image containing multiple fish (see details in Supporting Information, Fig. S2 D).

The high performance of SAM is largely attributed to the quality of the CavFish dataset and the PhotoFish system (García-Melo et al. 2019). Unlike databases such as FishBase (Froese and Pauly 2024) and FishNet (Khan et al. 2023), where image variability in specimen condition, background, lighting, and tank setup limits morphometric consistency, CavFish ensures taxonomically informative images that preserve natural shape and utilize controlled backgrounds. This minimizes segmentation variability and enhances model accuracy. Although SAM has not yet been tested on other datasets, as mentioned above, adopting standardized photographic protocols is strongly recommended to improve segmentation accuracy across in diverse field conditions.

The integration of SAM with CavFish allowed for a partially sampled evaluation of the morphometric diversity of Colombian freshwater fish, supporting previous findings on species-level morphological variation and its ecological significance. The morphospace of Colombian freshwater fish is dominated by a single high-density node, suggesting that most species share a common body shape (Fig. 2A) that is intermediate-sized with flattened, roughly elliptical bodies that are compressed either dorsoventrally or laterally. This morphology is commonly represented in world freshwater fishes, such as *Andinoacara latifrons* and *Lasiancistrus* spp. (Winemiller 1991; Su et al., 2018, Toussaint et al. 2016). The PC1 primarily reflects differences in overall body proportions, delineating a morphospace from larger species with rounded outlines to smaller, more streamlined shapes. PC2 captures variations in body perimeter, separating species with broader, irregular shapes, often associated with larger or more numerous fins, from those with more symmetrical bodies where fin structures are reduced. PC3 was most strongly associated with Zernike moment 1. This axis differentiates species with deeper, rounder body shapes, often bearing distinctive structures such as dorsal-fin filaments, from more streamlined species. In contrast, PC4, primarily associated with the Zernike moment 3, separates streamlined taxa with fin extensions, such as caudal-fin filaments, from highly elongate shapes.

Across the sampled Andean basins, body elongation emerges as the dominant axis of morphometric variation associated with locomotion and habitat use (Conde-Saldaña et al. 2017; Caillon et al. 2018). Elongated, fusiform, or streamlined body shapes are widely recognized adaptations for reducing drag and maximizing sustained swimming efficiency (Blake 2004; Langerhans 2009; Hincapié-Cruz

and Márquez 2021). These traits improve energy-efficient locomotion, making them advantageous for species inhabiting open-water environments or high-flow habitats (Langerhans and Reznick 2010). This pattern is consistent with classic ecomorphology in freshwater fishes, both in the Neotropics and globally, where elongation contrasts with deep body plans to reflect trade-offs between steady cruising and unsteady, maneuver-based performance (Winemiller 1991; Toussaint et al. 2016). At broader scales, global syntheses of morphological/functional diversity show that the Neotropics occupy unusually large portions of morphospace, much of it structured by dominant orders, including Characiformes and Siluriformes, providing a macroecological backdrop that aligns with our within-basin results (Toussaint et al. 2016). Taken together, these comparisons indicate that the axes we recover are not artefacts of sampling or methodology, but expressions of recurrent ecomorphological gradients observed across freshwater systems. As stated throughout, our inferences remain restricted to the basins, habitats, and taxa that were actually sampled.

In Colombian freshwater ecosystems, elongate species include *Ctenolucius hujeta* (Characiformes), *Farlowella mariae* (Siluriformes), *Potamorhaphis* spp., and *Belonion dibranchodon* (Atheriniformes), alongside *Synbranchus marmoratus* (Synbranchiformes). While many elongate forms conform to the expectation of enhanced sustained swimming, others, such as *Synbranchus marmoratus* and *Farlowella mariae*, depart from this pattern. Instead, elongation in *Synbranchus* is associated with fossorial habits and enhanced body flexibility, enabling these eels to exploit crevices, mud, and sand substrates (Claverie and Wainwright 2014). More broadly, body elongation also influences feeding strategies: deeper-bodied shapes often support greater suction performance due to the larger cross-sectional area of the epaxial musculature (Holzman et al. 2012), whereas highly elongated fishes with numerous vertebrae exhibit increased flexibility that may trade off with suction capacity but facilitates alternative ecological roles (Yamada et al. 2009).

In contrast, species with deeper, laterally compressed bodies and larger caudal peduncles are adapted for unsteady swimming, excelling in burst acceleration and maneuverability within structurally complex environments (Langerhans 2009). These traits are advantageous for rapid predator evasion and navigating through dense vegetation or heterogeneous habitats (Webb 1984; Schrank et al. 1999; Langerhans and Reznick 2010). Among Colombian freshwater fish, *Heros severus* and *Aequidens* spp. (Blenniiformes) and *Thoracocharax* spp. (Characiformes) exhibit these morphological features. This variation in body shape may have been the result of divergent selection pressures related to differences in water flow, dissolved oxygen availability, prey

abundance, and elevation gradient (Crispo and Chapman 2010; Foster et al. 2015; Malato et al. 2017).

The variation in fin morphology underscores the role of fins in body stabilization and locomotion. Previous ecomorphological studies of Neotropical fish have highlighted the functional importance of pectoral, pelvic, and caudal fins, particularly in relation to habitat exploitation under varying water velocities (Conde-Saldaña et al. 2017; Hulthén et al. 2024). Species with larger fins provide strong evidence that fin size plays a crucial role in generating escape momentum for predator avoidance (Gosline 1994; Hulthén et al. 2024). A notable example is *Hypostomus* spp. (Loricariidae), a group of Siluriformes commonly found in fast-flowing waters with rocky substrates (Conde-Saldaña et al. 2017). In contrast, species with smaller fins, such as *Knodus* spp. or *Astyanax* spp. (Characiformes) may benefit from reduced drag and enhanced maneuverability (Blake 2004; Langerhans 2009). This adaptation facilitates unstable swimming behaviors, characterized by frequent changes in velocity and direction (Webb 1982), allowing them to forage efficiently for food resources such as insects beneath macrophytes and submerged roots, which are common elements in Colombian freshwater ecosystems.

Similarly, we observe a continuous gradient, rather than distinct clusters, between contrasting locomotion strategies. This pattern reflects findings in other fish groups, such as reef fishes, where species tend to cluster densely in the central regions of trait space and gradually thin out toward the more specialized extremes (e.g., Mouillot et al. 2014). Within this continuum, Characiformes and Siluriformes, the most species-rich Neotropical orders (Lévêque et al. 2008; Nelson et al. 2016), contribute prominently to morphospace occupancy in our sample, spanning from deep-bodied, fin-rich outlines (e.g., *Serrasalmus hollandi*, Characiformes; *Heros severus*, Cichlidae) to elongated, streamlined shapes (e.g., *Ctenolucius hujeta*, Characiformes, and *Sturisomatichthys leightoni*, Siluriformes). At the periphery of the morphospace, Gymnotiformes (electric knifefishes) and Synbranchiformes (e.g., *Synbranchus marmoratus*) occupy highly specialized, extremely elongated regions. Peripheral positions in morphospace are typically occupied by species with unique or extreme body shapes that correspond to specialized functional roles. As a result, these species tend to exhibit greater functional vulnerability to loss. This pattern has been documented in both marine and freshwater fish assemblages, where morphologically extreme species are relatively uncommon yet contribute disproportionately to functional diversity (Mouillot et al. 2014; Su et al. 2019). By contrast, Blenniiformes (e.g., *Heros severus*) cluster in a localized zone of deep, laterally compressed bodies with expanded dorsal and anal rays, a configuration associated with unsteady swimming performance and maneuverability

in structurally complex habitats (Webb 1984; Langerhans 2009).

Beyond these ecological and functional interpretations, the observed body shape diversity also reflects deeper evolutionary processes. Natural selection drives morphological divergence through environmental adaptation, with water flow, habitat complexity, and predation pressure serving as the main forces shaping body plans suited to distinct ecological roles (Manna et al. 2017; Scharnweber 2020). Simultaneously, adaptive radiations, such as those seen in cichlids and loricariids, illustrate how the colonization of novel ecological niches can trigger rapid morphological diversification (Lujan and Armbruster 2012; Arbour and López-Fernández 2016). Furthermore, functional innovations, such as jaw specialization in Loricariidae or lower lip differentiation in Cyprinidae, have allowed certain lineages to access novel food resources, expanding their ecological breadth and contributing to morphospace expansion (Lujan and Armbruster 2012; Corse et al. 2015).

Finally, we adopted an AI-assisted pipeline based on standardized 2D field photographs to maximize non-lethal, low-cost, and logically feasible sampling across remote Colombian basins, in line with major neotropical trait resources that rely on lateral images (e.g., FishBase (Froese and Pauly 2024), Fish-AIR (Bakış et al. 2023), CaVFish). From these outlines, pose-invariant outline descriptors (Hu and Zernike moments) quantify whole-outline variation and recover the dominant ecomorphological gradients repeatedly reported in species-rich faunas (deep-bodied, elongate/streamlined) (Winemiller 1991; Conde-Saldaña et al. 2017; Caillon et al. 2018; Su et al. 2019). In contrast, linear-measurement morphospaces summarize only a small fraction of overall shape and, when variables mix scales, can yield non-metric distances (Price et al. 2019; Polly 2023). Our 2D approach, however, has several limitations: a lateral outline cannot capture dorsoventral relief, cross-sectional width, or positional traits (e.g., pectoral base, eye position) (Claude 2008; Torgersen et al. 2023). Width is functionally consequential (feeding, respiration, locomotion) (Webb 1982; Langerhans and Reznick 2010; Lujan and Armbruster 2012), and varies clearly in dorsoventrally compressed shapes (e.g., siluriform catfishes such as *Lasiancistrus* spp.). Although 3D photogrammetry and CT-based geometric morphometrics address these aspects by recovering volumetric and cross-sectional anatomy (e.g., (Torgersen et al. 2023), they remain costlier, logically demanding, and often depend on preserved material, introducing shape body distortion and reducing field coverage. Accordingly, we present our 2D pipeline as a baseline optimized for broad geographic and taxonomic coverage of Colombia's ichthyofauna, while clearly defining its scope. Moving forward, species representation should be expanded beyond the four

Andean basins included in this study, which are currently skewed towards Characiformes, Siluriformes, and Blenniiformes. Future efforts should also incorporate additional localized traits, such as eye position, dentition, gill-raker and fin morphology, caudal peduncle structure, and head/mouth shape. Finally, the implementation of 3D analyses would allow the inclusion of an additional axis of ecologically relevant shape variation.

## Conclusions

This study demonstrates the effectiveness of AI-driven segmentation using foundation models for large-scale morphometric analysis of Colombian freshwater fish, representing the first application of a deep learning pipeline to quantify morphological diversity directly from standardized field photography of live specimens. Using Segment Anything's (SAM) zero-shot segmentation capability, our workflow achieves 97% segmentation accuracy, accurately delineating fish morphology across a wide range of body shapes and sizes. These results establish SAM's capacity to replace manual segmentation, dramatically reducing annotation effort while preserving the precision required for quantitative morphological analyses.

Our study provides the first broad, field-based assessment of morphometric diversity in Colombian freshwater fishes using standardized images of live specimens. The ichthyofaunal composition represented in this dataset reveals a predominant compressed morphotype consistent with generalized swimming and habitat use. Clear order-level differences are readily observed: Synbranchiformes show a distinctive elongate shape, whereas Characiformes and Siluriformes span deep-bodied, streamlined, elongate, dorsoventrally flattened, and elaborate fin morphotypes.

Importantly, our workflow enables the scalable, noninvasive, and standardized collection of morphometric data from living organisms in natural environments. This methodology offers a scalable and efficient solution for researchers. By facilitating rapid, high-throughput analyses of morphological traits, this contribution not only addresses current limitations in data availability but also opens avenues for the advancement of comparative morphology, functional ecology, evolutionary drivers of variation, and ecosystem monitoring in freshwater systems.

**Supplementary Information** The online version contains supplementary material available at <https://doi.org/10.1007/s00435-025-00747-x>.

**Acknowledgements** We thank the Field Museum of Chicago, WWF, Fundación Omacha, Universidad del Tolima, and Universidad de Ibagué for their support during expeditions that allowed the photographic documentation of Colombian fish species. We also acknowledge the

Universidad Industrial de Santander, particularly the School of Biology, for their funding and assistance in this research. Likewise, the Biomedical Imaging, Vision and Learning Laboratory (BIVL2ab), Biotechnology and Environmental Management Research Group (iBGA), Imageomics Institute and the CavFish Scientific Committee provided computational resources, species identification, and valuable insights. Special thanks to Marlon Camilo Herrera for his dedication to the Visual Science Lab. The authors wish to thank anonymous reviewers, and the editors for their valuable revisions to improve the manuscript. This work was supported by the Universidad Industrial de Santander, Colombia, through a forgivable loan for doctoral studies in Biological Sciences awarded to Jose Luis Poveda Cuellar.

**Author contributions** All authors contributed to the conception, design, and interpretation of the research, integrating their perspectives according to their areas of expertise. Efforts were made to consider the scientific literature relevant to Colombia. Data analysis was performed by JLPC; DMD; and FMC, who also participated along with JGM; SM; and BR contributed the review and preparation of the manuscript. Fish photographs were taken by JEGM using the Photafish system and archived in the CavFish database. The manuscript was primarily written by JLPC and DMD. All authors approved the final manuscript.

**Funding** Open Access funding provided by Colombia Consortium. This work was supported by the Universidad Industrial de Santander, Colombia, through a forgivable loan for doctoral studies in Biological Sciences awarded to Jose Luis Poveda Cuellar.

**Data availability** Data supporting the findings of this study are openly available on the CavFish-Colombia platform (<https://cavfish.unibague.edu.co/catalogo>) upon reasonable request. The analysis code is hosted on GitHub and has also been archived in Harvard Dataverse: <https://doi.org/10.7910/DVN/GR5J6S>, Harvard Dataverse, V1.

## Declarations

**Conflict of interest** The authors declare no competing interests.

**Ethical approval** Ethical approval was not required for this study, as no experiments involving live animals were conducted. All images used were sourced from the CavFish Colombia project.

**Open Access** This article is licensed under a Creative Commons Attribution 4.0 International License, which permits use, sharing, adaptation, distribution and reproduction in any medium or format, as long as you give appropriate credit to the original author(s) and the source, provide a link to the Creative Commons licence, and indicate if changes were made. The images or other third party material in this article are included in the article's Creative Commons licence, unless indicated otherwise in a credit line to the material. If material is not included in the article's Creative Commons licence and your intended use is not permitted by statutory regulation or exceeds the permitted use, you will need to obtain permission directly from the copyright holder. To view a copy of this licence, visit <http://creativecommons.org/licenses/by/4.0/>.

## References

- Arbour JH, López-Fernández H (2016) Continental cichlid radiations: functional diversity reveals the role of changing ecological opportunity in the neotropics. Proc R Soc B 283:20160556. <https://doi.org/10.1098/rspb.2016.0556>

- Ariede RB, Lemos CG, Batista FM et al (2023) Computer vision system using deep learning to predict rib and loin yield in the fish *Colossoma macropomum*. Anim Genet 54:375–388. <https://doi.org/10.1111/age.13302>
- Bakış Y, Wang X, Altıntaş B et al (2023) On image quality metadata, FAIR in ML, AI-readiness and reproducibility: fish-AIR example. BISS 7:e112178. <https://doi.org/10.3897/biss.7.112178>
- Barragán KS, Chuctaya J, Escobar-Camacho D et al (2024) Fresh vs. preserved specimens: length-weight relationships of fishes from the Western Amazon (Napo Basin, Ecuador). J Appl Ichthyol 2024:2430326. <https://doi.org/10.1155/2024/2430326>
- Blake RW (2004) Fish functional design and swimming performance. J Fish Biol 65:1193–1222. <https://doi.org/10.1111/j.0022-1112.2004.00568.x>
- Bloch M (1795) Naturgeschichte der ausländischen Fische. Berlin. v. 9: i-ii + 1-192, Pls. 397-429. [Also a French edition, Ichthyologie, ou Histoire naturelle, générale et particulière des poissons, v. 12, published 1797.]
- Cailliet F, Bonhomme V, Möllmann C, Frelat R (2018) A morphometric dive into fish diversity. Ecosphere 9:e02220. <https://doi.org/10.1002/ecs2.2220>
- Carmona CP, Pavanetto N, Puglielli G (2024) Funspace: an R package to build, analyse and plot functional trait spaces. Divers Distrib 30:e13820. <https://doi.org/10.1111/ddi.13820>
- Claude J (2008) Morphometrics with R. Springer, New York
- Claverie T, Wainwright PC (2014) A morphospace for reef fishes: elongation is the dominant axis of body shape evolution. PLoS ONE 9:e112732. <https://doi.org/10.1371/journal.pone.0112732>
- Collette B (1966) Belonion, a new genus of fresh-water needlefishes from South America. Am Mus Novit 2274:1–22
- Conde-Saldaña CC, Albornoz-Garzón JG, López-Delgado EO, Villa-Navarro FA (2017) Ecomorphological relationships of fish assemblages in a trans-Andean drainage, upper Magdalena river Basin, Colombia. Neotrop Ichthyol. <https://doi.org/10.1590/1982-0224-20170037>
- Corse E, Tarkan AS, Emiroğlu Ö et al (2015) Covariation of trophic and habitat-related traits in chondrostomes (Cyprinidae): implications for repeated and diversifying evolutionary processes. J Zool 295:294–305. <https://doi.org/10.1111/jzo.12212>
- Crispo E, Chapman LJ (2010) Geographic variation in phenotypic plasticity in response to dissolved oxygen in an African cichlid fish. J Evolut Biol 23:2091–2103. <https://doi.org/10.1111/j.1429-9101.2010.02069.x>
- Cuvier G, Valenciennes A (1850) Histoire naturelle des poissons. Tome vingt-deuxième. Suite du livre vingt-deuxième. Suite de la famille des Salmonoïdes. Table générale de l'Histoire Naturelle des Poissons (pp. 1–91). v. 22: i-xx + 1 p. + 1-532 + 1-91, Pls. 634–650. [Valenciennes authored volume. Published as "1849". i-xvi + 1-395, index 1-81 (+ 1) in Strasbourg edition.]
- DoNascimiento C, Agudelo-Zamora HD, Bogota-Gregory JA (2024) Lista de especies de peces de agua dulce de Colombia/checklist of the freshwater fishes of Colombia.v2.17. <https://doi.org/10.15472/numrso>
- Duong T (2007) Ks: kernel density estimation and kernel discriminant analysis for multivariate data in R. J Stat Soft. <https://doi.org/10.18637/jss.v021.i07>
- Eigenmann C, Bray W (1894) A revision of the American Cichlidae. Ann New York Acad Sci 7(art. 4):607–624
- Eigenmann C (1915) The Serrasalminae and Myliinae. Ann Carnegie Museum 9(3–4):226–272, Pls. 44–58
- Fernandes AFA, Turra EM, De Alvarenga ÉR et al (2020) Deep learning image segmentation for extraction of fish body measurements and prediction of body weight and carcass traits in Nile tilapia. Comput Electron Agric 170:105274. <https://doi.org/10.1016/j.compag.2020.105274>
- Foster K, Bower L, Piller K (2015) Getting in shape: habitat-based morphological divergence for two sympatric fishes: habitat-based morphological divergence. Biol J Linn Soc Lond 114:152–162. <https://doi.org/10.1111/bij.12413>
- Froese R, Pauly D (2024) FishBase. World Wide Web electronic publication. <https://www.fishbase.se/search.php>. Accessed 11 Aug 2024
- Garcia-d'Urso N, Galan-Cuenca A, Pérez-Sánchez P et al (2022) The deepfish computer vision dataset for fish instance segmentation, classification, and size estimation. Sci Data 9:287. <https://doi.org/10.1038/s41597-022-01416-0>
- García-Melo JE, García-Melo LJ, García-Melo JD et al (2019) Photafish system: an affordable device for fish photography in the wild. Zootaxa. <https://doi.org/10.11646/zootaxa.4554.1.4>
- Gatz AJ (1979) Community organization in fishes as indicated by morphological features. Ecology 60:711–718
- Gonzalez RC, Woods RE (2018) Digital image processing. Pearson, New York
- Gosline WA (1994) Function and structure in the paired fins of scorpaeniform fishes. Environ Biol Fish 40:219–226. <https://doi.org/10.1007/BF00002508>
- Günther A (1864) Catalogue of the fishes in the British Museum. Catalogue of the Physostomi, containing the families Siluridae, Characidae, Haplochitonidae, Sternopychidae, Scopelidae, Stomiataidae in the collection of the British Museum. v. 5: i-xxii + 1–455
- Han B, Hu Z, Su Z et al (2022) Mask\_LaC R-CNN for measuring morphological features of fish. Measurement 203:111859. <https://doi.org/10.1016/j.measurement.2022.111859>
- Hasegawa T, Nakano D (2024) Robust fish recognition using foundation models toward automatic fish resource management. JMSE. <https://doi.org/10.3390/jmse12030488>
- Heckel J (1840) Johann Natterer's neue Flussfische Brasilien's nach den Beobachtungen und Mittheilungen des Entdeckers beschrieben (Erste Abtheilung, Die Labroiden). Annalen des Wiener Museums der Naturgeschichte 2:325–471, Pls. 29–30
- Helser TE, Benson I, Erickson J et al (2019) A transformative approach to ageing fish otoliths using fourier transform near infrared spectroscopy: a case study of eastern bering sea walleye pollock (*Gadus chalcogrammus*). Can J Fish Aquat Sci 76:780–789. <https://doi.org/10.1139/cjfas-2018-0112>
- Hernández-Serna A, Jiménez-Segura LF (2014) Automatic identification of species with neural networks. PeerJ 2:e563. <https://doi.org/10.7717/peerj.563>
- Hincapié-Cruz JP, Márquez EJ (2021) Variación fenotípica de los peces *Curimata mivartii* (Characiformes: Curimatidae) y *Pimelodus grosskopffii* (Siluriformes: Pimelodidae) en hábitats lóticos y lénicos. Revista De Biología Trop 69
- Holzman R, Collar DC, Mehta RS, Wainwright PC (2012) An integrative modeling approach to elucidate suction-feeding performance. J Exp Biol 215:1–13. <https://doi.org/10.1242/jeb.057851>
- Hong Y, Zhou X, Hua R et al (2024) WaterSAM: Adapting SAM for underwater object segmentation. JMSE 12:1616. <https://doi.org/10.3390/jmse12091616>
- Hu (1962) Visual pattern recognition by moment invariants. IEEE Trans Inform Theory 8:179–187. <https://doi.org/10.1109/TIT.1962.1057692>
- Hulthén K, Vinterstare J, Nilsson PA, Brönmark C (2024) Finotypic plasticity: Predator-induced plasticity in fin size, darkness and display behaviour in a teleost fish. J Anim Ecol 93:1135–1146. <https://doi.org/10.1111/1365-2656.14130>
- Khan FF, Li X, Temple AJ, Elhoseiny M (2023) FishNet: a large-scale dataset and Benchmark for fish recognition, detection, and functional trait prediction. In: 2023 IEEE/CVF international conference on computer vision (ICCV). IEEE, Paris, France, p 20439–20449

- Kirillov A, Mintun E, Ravi N et al (2023) Segment anything. In: 2023 IEEE/CVF international conference on computer vision (ICCV). IEEE, Paris, France, p 3992–4003
- Langerhans RB (2009) Trade-off between steady and unsteady swimming underlies predator-driven divergence in *Gambusia affinis*. *J Evolut Biol* 22:1057–1075. <https://doi.org/10.1111/j.1420-9101.2009.01716.x>
- Langerhans RB, Reznick DN (2010) Ecology and evolution of swimming performance in fishes: predicting evolution with biomechanics. In: Domenici P, Kapoor BG (eds) Fish locomotion, 1st edn. CRC, pp 200–248
- Lévêque C, Oberdorff T, Paugy D et al (2008) Global diversity of fish (Pisces) in freshwater. *Hydrobiologia* 595:545–567. <https://doi.org/10.1007/s10750-007-9034-0>
- Liu S, Zeng Z, Ren T et al (2024) Grounding DINO: marrying DINO with grounded pre-training for open-set object detection. <https://doi.org/10.48550/arXiv.2303.05499>
- Lujan NK, Armbruster JW (2012) Morphological and functional diversity of the mandible in sucker-mouth armored catfishes (Siluriformes: Loricariidae). *J Morphol* 273:24–39. <https://doi.org/10.1002/jmor.11003>
- Malato G, Shervette VR, Navarrete Amaya R et al (2017) Parallel body shape divergence in the Neotropical fish genus *Rhoadsia* (Teleostei: Characidae) along elevational gradients of the Western slopes of the Ecuadorian Andes. *PLoS ONE* 12:e0179432. <https://doi.org/10.1371/journal.pone.0179432>
- Manna LR, Rezende CF, Mazzoni R (2017) Effect of body size on microhabitat preferences in stream-dwelling fishes. *J Appl Ichthyol* 33:193–202. <https://doi.org/10.1111/jai.13320>
- Martinez PA, Berbel-Filho WM, Jacobina UP (2013) Is formalin fixation and ethanol preservation able to influence in geometric morphometric analysis? Fishes as a case study. *Zoomorphology* 132:87–93. <https://doi.org/10.1007/s00435-012-0176-x>
- Martín Salazar F (1964) Las especies del género Farlowella de Venezuela (Piscis [sic] - Nematognalhi [sic] - Loricariidae) con descripción de 5 especies y 1 sub-especie nuevas. Memoria de la Sociedad de Ciencias Naturales La Salle 24(69):242–260
- Mouillet D, Villéger S, Parravicini V et al (2014) Functional over-redundancy and high functional vulnerability in global fish faunas on tropical reefs. *Proc Natl Acad Sci USA* 111:13757–13762. <https://doi.org/10.1073/pnas.1317625111>
- Nelson JS, Grande TC, Wilson MV (2016) Fishes of the World. Wiley
- Ou L, Liu B, Chen X et al (2023) Automated identification of morphological characteristics of three *Thunnus* species based on different machine learning algorithms. *Fishes* 8:182. <https://doi.org/10.3390/fishes8040182>
- Paszke A, Gross S, Massa F et al (2019) PyTorch: an imperative style, high-performance deep learning library. In: Wallach H, Larochelle H, Beygelzimer A et al (eds) Advances in neural information processing systems. Curran Associates, Inc
- Pelicice FM, Agostinho AA, Azevedo-Santos VM et al (2023) Ecosystem services generated by neotropical freshwater fishes. *Hydrobiologia* 850:2903–2926. <https://doi.org/10.1007/s10750-022-04986-7>
- Petrellis N (2021) Measurement of fish morphological features through image processing and deep learning techniques. *Appl Sci* 11:4416. <https://doi.org/10.3390/app11104416>
- Polly PD (2023) Extinction and morphospace occupation: a critical review. *Camb Prisms Extinct* 1:e17. <https://doi.org/10.1017/ext.2023.16>
- Price SA, Friedman ST, Corn KA et al (2019) Building a body shape morphospace of teleostean fishes. *Integr Comp Biol* 59:716–730. <https://doi.org/10.1093/icb/icz115>
- Rocha WS, Da Fonseca TFC, Watanabe CYV et al (2024) Automatic measurement of fish from images using convolutional neural networks. *Multimed Tools Appl*. <https://doi.org/10.1007/s11042-024-19180-1>
- Sabaj Pérez MH (2009) Photographic atlas of fishes of the Guiana shield. *Bull Biol Soc Wash* 17:52–59. <https://doi.org/10.2988/0097-0298-17.1.52>
- Saleh A, Jones D, Jerry D, Azghadi MR (2023) MFLD-net: a lightweight deep learning network for fish morphometry using landmark detection. *Aquat Ecol* 57:913–931. <https://doi.org/10.1007/s10452-023-10044-8>
- Scharnweber K (2020) Morphological and trophic divergence of lake and stream minnows (*Phoxinus phoxinus*). *Ecol Evol* 10:8358–8367. <https://doi.org/10.1002/ece3.6543>
- Schneider J, Meske C, Kuss P (2024) Foundation models: A new paradigm for artificial intelligence. *Bus Inf Syst Eng* 66:221–231. <https://doi.org/10.1007/s12599-024-00851-0>
- Schrank AJ, Webb PW, Mayberry S (1999) How do body and paired-fin positions affect the ability of three teleost fishes to maneuver around bends? 77:203–210. <https://doi.org/10.1139/z98-209>
- Sigurðardóttir AR, Sveinsdóttir HI, Schultz N et al (2024) Sequence segmentation of nematodes in Atlantic Cod with multispectral imaging data. *Foods* 13:2952. <https://doi.org/10.3390/foods13182952>
- Sotola VA, Craig CA, Pfaff PJ et al (2019) Effect of preservation on fish morphology over time: implications for morphological studies. *PLoS ONE* 14:e0213915. <https://doi.org/10.1371/journal.pone.0213915>
- Su G, Villéger S, Brosse S (2019) Morphological diversity of freshwater fishes differs between realms, but morphologically extreme species are widespread. *Global Ecol Biogeogr* 28:211–221. <https://doi.org/10.1111/geb.12843>
- Tonella LH, Ruaro R, Daga VS et al (2023) NEOTROPICAL FRESHWATER FISHES: A dataset of occurrence and abundance of freshwater fishes in the neotropics. *Ecology* 104:e3713. <https://doi.org/10.1002/ecy.3713>
- Torgersen KT, Bouton BJ, Hebert AR et al (2023) Phylogenetic structure of body shape in a diverse inland ichthyofauna. *Sci Rep* 13:20758. <https://doi.org/10.1038/s41598-023-48086-5>
- Toussaint A, Charpin N, Brosse S, Villéger S (2016) Global functional diversity of freshwater fish is concentrated in the Neotropics while functional vulnerability is widespread. *Sci Rep* 6:22125. <https://doi.org/10.1038/srep22125>
- Tseng C-H, Hsieh C-L, Kuo Y-F (2020) Automatic measurement of the body length of harvested fish using convolutional neural networks. *Biosyst Eng* 189:36–47. <https://doi.org/10.1016/j.biosystemseng.2019.11.002>
- Webb PW (1982) Locomotor patterns in the evolution of actinopterygian fishes. *Am Zool* 22:329–342
- Webb PW (1984) Body form, locomotion and foraging in aquatic vertebrates. *Am Zool* 24:107–120
- Winemiller KO (1991) Ecomorphological diversification in lowland freshwater fish assemblages from five biotic regions. *Ecol Monogr* 61:343–365. <https://doi.org/10.2307/2937046>
- Yamada T, Sugiyama T, Tamaki N et al (2009) Adaptive radiation of gobies in the interstitial habitats of gravel beaches accompanied by body elongation and excessive vertebral segmentation. *BMC Evol Biol* 9:145. <https://doi.org/10.1186/1471-2148-9-145>
- Yu C, Fan X, Hu Z et al (2020) Segmentation and measurement scheme for fish morphological features based on mask R-CNN. *Inform Process Agric* 7:523–534. <https://doi.org/10.1016/j.inpa.2020.01.002>
- Zhuang F, Qi Z, Duan K et al (2021) A comprehensive survey on transfer learning. *Proc IEEE* 109:43–76. <https://doi.org/10.1109/JPROC.C.2020.3004555>